

**Table I.** Unimolecular Rate Constants ( $s^{-1}$ ) for Hopping

T, K	H			D		
	CHO	VVD	present	CHO	VVD	present
120	$9.0 \times 10^{-8}$	$3.5 \times 10^{-5}$	$2.5 \times 10^{-5}$	$6.3 \times 10^{-8}$	$1.5 \times 10^{-6}$	$7.8 \times 10^{-7}$
140	$9.2 \times 10^{-5}$	$7.1 \times 10^{-3}$	$4.4 \times 10^{-3}$	$6.5 \times 10^{-5}$	$6.4 \times 10^{-4}$	$4.2 \times 10^{-4}$
160	$1.7 \times 10^{-2}$	$4.6 \times 10^{-1}$	$3.2 \times 10^{-1}$	$1.2 \times 10^{-2}$	$6.6 \times 10^{-2}$	$5.0 \times 10^{-2}$
200	$2.4 \times 10^1$	$1.9 \times 10^2$	$1.7 \times 10^2$	$1.7 \times 10^1$	$5.0 \times 10^1$	$4.4 \times 10^1$
400	$5.2 \times 10^7$	$8.0 \times 10^7$	$8.6 \times 10^7$	$3.7 \times 10^7$	$4.4 \times 10^7$	$4.6 \times 10^7$
600	$6.7 \times 10^9$	$7.6 \times 10^9$	$8.4 \times 10^9$	$4.7 \times 10^9$	$4.8 \times 10^9$	$5.2 \times 10^9$
1000	$3.3 \times 10^{11}$	$3.2 \times 10^{11}$	$3.6 \times 10^{11}$	$2.3 \times 10^{11}$	$2.2 \times 10^{11}$	$2.5 \times 10^{11}$

**Table II.** Factors Contributing to the Ratio of the Present Hopping Rate Constant to the CHO Results for H

T, K	anharmonicity	bound-mode quantization	tunneling	total
120	0.83	22.1	15.3	280.
140	0.85	11.7	4.8	47.9
160	0.87	7.4	2.9	19.0
200	0.89	4.1	1.88	6.8
400	0.95	1.52	1.15	1.65

potential of Gregory et al.<sup>15</sup> The activated diffusion process consists of hopping between fourfold coordination sites (binding energy BE = 40.2 kcal/mol; distance from surface plane  $z = 1.14$  Å). The saddlepoint is a two-fold bridge site (BE = 28.6 kcal/mol,  $z = 1.68$  Å). The polyatomic version of the reaction-path Hamiltonian,<sup>10,14,16</sup> canonical variational transition-state theory,<sup>8-10,17</sup> and the small-curvature-approximation SAG transmission coefficient<sup>9,10,18</sup> are generalized to the case of an adsorbate on a surface and are used to calculate a unimolecular site-to-nearest-site hopping rate constant  $k$ ; anharmonicity is included by the independent-normal-mode<sup>10,17</sup> and WKB<sup>13</sup> approximations, and the small-curvature approximation accounts for the nonrectilinear multidimensional nature of the tunneling path, involving motion both parallel and perpendicular to the surface. The hopping rate constant can be converted to a two-dimensional diffusion coefficient under the assumption of uncorrelated hops<sup>19</sup> by multiplying by  $l^2/4$ , where  $l$  is the hop length (2.624 Å).

The calculated hopping rate constants (including a factor of 4 for the number of equivalent hopping directions) are given in Table I, where they are compared to the results of VVD and to another set of calculations performed by us in which we neglected anharmonicity, quantization of bound vibrational modes, and tunneling. The latter calculation is abbreviated CHO (classical harmonic oscillator). Table I shows excellent agreement among the various methods at high  $T$ , but the two semiclassical rate constants are appreciably higher than the CHO result at low temperature. Considering the large deviations of these two sets of results from the CHO ones and also the fact that the three responsible effects (anharmonicity, bound-mode quantal effects, and tunneling) are implicit in the VVD work only through the effective potential, but are treated explicitly and separately by quite different methods in our work, the agreement of the two sets of semiclassical results within a factor of 1.6 for  $T \geq 140$  K and 1.9 for  $T = 120$  K is quite encouraging.

Table II shows the three separate effects for surface diffusion of H. The last column is the ratio of the present rate constants to the CHO ones, and this ratio is a product of the first three factors. This table shows that the two quantal effects are more important than anharmonicity. Furthermore tunneling increases the rate by factors of 3-15 at 160-120 K and therefore greatly dominates the over-the-barrier contributions at these temperatures.

Primarily because of the tunneling contribution the present calculations show two of the same qualitative features present in

the low-temperature experiments of DiFoggio and Gomer.<sup>2,3</sup> First, the kinetic isotope effects greatly exceed the classical value of 1.4. Second, the Arrhenius plots become quite nonlinear at low temperature, with the deviation from the extrapolation of the high-temperature Arrhenius fit roughly comparable to the tunneling factor. An Arrhenius fit at 1000 K yields activation energies of 11.4 and 11.6 kcal/mol and preexponential factors of  $1.12 \times 10^{14}$  and  $8.31 \times 10^{13} s^{-1}$  for H and D, respectively. However, the activation energies decrease to 7.6 and 10.4 kcal/mol at 120 K.

We draw three significant conclusions from the present study: (i) The Gaussian-averaged effective potential method<sup>5-7</sup> appears to be a reasonably accurate way to incorporate quantal effects into many-body molecular dynamics simulations. (ii) The reaction-path formulation of variational transition-state theory with semiclassical transmission coefficients appears to be a practical and accurate method for calculating surface diffusion coefficients and, as a corollary, probably also for calculating bulk diffusion coefficients,<sup>20</sup> even for hydrogen atoms when quantal effects are very large. (iii) Tunneling does appear to provide the dominant mechanism for low-temperature surface diffusion of H on metals.

**Acknowledgment.** We thank Steve Valone, Art Voter, and Jim Doll for providing preprints, a subprogram, and many helpful discussions. This work was supported in part by the U.S. Department of Energy, Office of Basic Energy Sciences, through Contract DOE/DE-AC02-79ER10425.

**Registry No.** H<sub>2</sub>, 1333-74-0; Cu, 7440-50-8; D<sub>2</sub>, 7782-39-0.

(20) Tunneling has also been invoked to explain bulk diffusion of H in metals, which is of great technological interest. See, e.g.: Alefield, G. *Comments Solid State Phys.* 1975, 6, 53.

## Facile Oxidation of Methoxide to Formaldehyde by a Heterocyclic Quinone

Edward B. Skibo\* and Chang Hee Lee

Department of Chemistry, Arizona State University  
Tempe, Arizona 85287

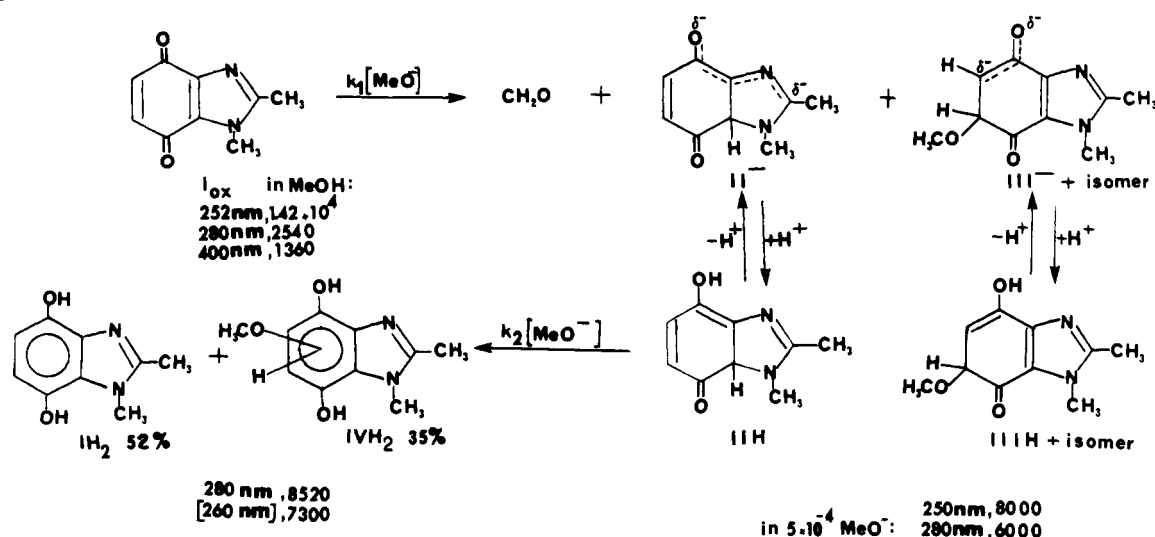
Received February 20, 1985

The oxidation of conjugated alcohols to the corresponding carbonyl derivatives by high redox potential quinones is well documented.<sup>1,2</sup> The postulated mechanism involves hydride transfer from the neutral alcohol to the quinone providing an oxocarbenium ion stabilized by conjugation and the hydroquinone anion.<sup>1,2a</sup> Rapid proton loss from the former species then provides the carbonyl product. Thus, the high-energy oxocarbenium ion which would arise from methanol precludes its oxidation by

- (15) Gregory, A. R.; Gelb, A.; Silbey, R. *Surf. Sci.* 1979, 74, 497.  
 (16) Miller, W. H.; Handy, N. C.; Adams, J. E. *J. Chem. Phys.* 1980, 72, 99.  
 (17) Isaacson, A. D.; Truhlar, D. G. *J. Chem. Phys.* 1982, 76, 1380.  
 (18) Skodje, R. T.; Garrett, B. C.; Truhlar, D. G. *J. Phys. Chem.* 1981, 85, 3019.  
 (19) Voter, A. F.; Doll, J. D. *J. Chem. Phys.* 1984, 80, 5832.

- (1) (a) Braude, E. A.; Linstead, R. P.; Wooldridge, K. R. *J. Chem. Soc.* 1956, 3070. (b) Warren, C. K.; Weedon, B. C. L. *J. Chem. Soc.* 1958, 3972. (c) Crombie, L.; Ellis, J. A.; Gould, R.; Pattenden, G.; Elliot, M.; Janes, N. F.; Jeffs, K. A. *J. Chem. Soc. C* 1971, 9. (d) Burn, D.; Petrov, V.; Weston, G. O. *Tetrahedron Lett.* 1960, 14. (e) Pilling, G. M.; Sondheimer, F. *J. Am. Chem. Soc.* 1971, 93, 1977. (f) Becker, H.-D.; Adler, E. *Acta Chem. Scand.* 1961, 15, 218. (g) Becker, H.-D.; Bremholt, T. *Tetrahedron Lett.* 1973, 197. (h) Brown, D. R.; Turner, A. B. *J. Chem. Soc., Perkin Trans. 2* 1975, 1307. (2) Ohki, A.; Nishiguchi, T.; Fukuzumi, K. *Tetrahedron* 1979, 35, 1737.

Scheme I



quinones and even permits its use as a reaction solvent for quinone-mediated oxidations. Yet bacterial methanol dehydrogenase effectively catalyzes the oxidation of methanol employing a heterocyclic quinone cofactor.<sup>3</sup> Queries posed are thus the manner by which methanol becomes activated toward quinone-mediated oxidation and the mechanistic details of oxidation. Discussed herein is the facile oxidation of methoxide in methanol to formaldehyde by 1,2-dimethylbenzimidazole-4,7-dione ( $I_{ox}$ ),<sup>4</sup> Scheme I. We consider that a hydride-transfer mechanism is in operation based on the mechanism proposed for the quinone-mediated oxidation of other alcohols and on the experimental findings cited below. That hydride transfer could occur to a carbonyl oxygen<sup>1,2a</sup> rather than to a carbon center bearing a partial positive charge is not considered, however. We prefer a two-step process for hydroquinone formation: hydride transfer to a carbon center followed by enolization. Thus, hydride transfer from methoxide to  $I_{ox}$  yields a spectrally observable 7a-hydrido adduct ( $IIH_T = II^- + IIH$ ) and formaldehyde which is followed by methoxide-catalyzed enolization of the former species to the hydroquinone ( $I_{H_2T} = I_{H_2} + \text{ionic forms}$ ). A parallel reaction is methoxide addition at the 5- and 6-positions of  $I_{ox}$  to provide adducts ( $IIIH_T = IIH + III^-$ ) which undergo methoxide-catalyzed enolization to the methoxylated hydroquinones ( $IV_{H_2T} = IV_{H_2} + \text{ionic forms}$ ). Paradoxical, considering the facility of oxidation, is the estimated two-electron redox potential range of -200 to -300 mV (vs. NHE) for  $I_{ox}/I_{H_2T}$  in basic media. This estimate is based on a fit of  $E_m$  vs. pH data for the above redox couple ( $\mu = 1.0$  with  $KClO_4$  at 25 °C in aqueous buffer) to the Nernst equation. The driving force for oxidation is seen as originating from both the high free energy of methoxide (pKa 16.7) and the stabilization of  $II^-$  by delocalization of the anion into the fused imidazole ring. In conclusion, the unstable oxocarbenium ion intermediate arising by hydride transfer from methanol is avoided by transferring the proton first and then hydride. Also, heterocyclic quinone systems in general may facilitate hydride acceptance by delocalization of charge into electron-deficient fused rings.

The reaction of methoxide with  $I_{ox}$  was studied at  $30 \pm 0.2$  °C in strictly anaerobic methanol under the pseudo-first-order conditions of  $[I_{ox}] = 5 \times 10^{-5}$  M  $\ll$   $[MeO^-] = 5 \times 10^{-4}$  to  $5 \times 10^{-3}$  M. By following the course of the reaction spectrophotometrically (252 or 280 nm), two consecutive first-order changes in absorbance were noted. Rate constants and extinction coefficients were obtained by fitting OD vs.  $t(s)$  data to a two-exponential absorbance equation.<sup>5</sup> The rate laws for both the first and second phases

were seen to be first order in  $[MeO^-]$  and  $[I_{ox}]$  with  $k_1 = 46$  M<sup>-1</sup> s<sup>-1</sup> and  $k_2 = 6.6$  M<sup>-1</sup> s<sup>-1</sup>, respectively. A preparative reaction mixture consisting of  $1.5 \times 10^{-4}$  M  $I_{ox}$  and  $1.5 \times 10^{-3}$  M methoxide yielded 41%  $I_{ox}$  when the completed reaction was reoxidized and the product isolated and purified. The <sup>1</sup>H NMR of the crude unoxidized product in  $Me_2SO-d_6$  was that of authentic  $I_{H_2}$ . However, it was possible to isolate a mixture of 5- and 6-methoxylated derivatives of  $I_{ox}$  from the crude reoxidized product (~35% yield). The detection and assay of the formaldehyde accompanying  $I_{H_2T}$  formation was accomplished with the Hantzsch<sup>6</sup> reagent; the average yield obtained from repeat experiments was  $52 \pm 7\%$ . These products are proposed to form by competitive hydride and methoxide transfer as depicted in Scheme I. Employing the yield of formaldehyde, the second-order rate constants for hydride transfer and enolization are calculated as  $k_1 = 24$  M<sup>-1</sup> s<sup>-1</sup> and  $k_2 = 3.4$  M<sup>-1</sup> s<sup>-1</sup>. Consistent with the hydride-transfer mechanism, the yield of formaldehyde in methoxide/methanol- $d_4$  was only 28% and associated with the kinetic isotope effects of  $k_1(H)/k_1(D) = 3.7$  and  $k_2(H)/k_2(D) = 2.4$ . Reactions carried out in methoxide/methanol- $d_4$  did not result in observable deuterium incorporation at the 5- and 6-positions of the product or at the 2-position when the 2-unsubstituted analogue of  $I_{ox}$ <sup>7</sup> was employed. Thus hydride transfer to the 5- and 6-positions, like methoxide transfer, does not constitute a major pathway. These observations and the potential for anion stabilization suggest the formation of a 7a-adduct by either hydride or methoxide attack at this position. The latter may occur in a rapid equilibrium step but is not seen as being on the oxidation path (loc. cit., isotope effects). Hydride transfer to a carbonyl carbon, on the other hand, will result in a localized anion and is thus inconsistent with the facility of the reaction. Indeed the hydride transfer from methoxide to the carbonyl carbon of benzaldehyde occurs at only  $7.4 \times 10^{-6}$  M<sup>-1</sup> s<sup>-1</sup> at 100 °C!<sup>8</sup>

Aspects of the oxidation mechanism depicted in Scheme I have parallels in the literature. Swain and co-workers<sup>8</sup> have documented the formation of formaldehyde by hydride transfer from methoxide to benzaldehyde. Also, Farnig and Bruce<sup>9</sup> have documented carbon-carbon double-bond formation by hydride transfer from a carbanion to 5-carbalumiflavin. Other mechanistic possibilities involving the transfer of a hydride equivalent (sequential hydrogen atom<sup>10</sup> and radical transfer from methoxide) have not been rigorously disproven. An initial electron transfer from methoxide

(6) Nash, T. *Biochemistry* **1953**, *55*, 416.

(7) 1(2)-Methylbenzimidazole-4,7-dione yielded 58% reoxidized hydroquinone and 45–75% formaldehyde in a preparative study in methoxide/methanol.

(8) Swain, C. G.; Powell, A. L.; Lynch, T. J.; Alpha, S. R.; Dunlap, R. P. *J. Am. Chem. Soc.* **1979**, *101*, 3584.

(9) Farnig, O. L.; Bruce, T. C. *J. Chem. Soc., Chem. Commun.* **1984**, 185.

(10) Boyle, W. J.; Bunnett, J. F. *J. Am. Chem. Soc.* **1974**, *96*, 1418.

(3) Duine, J. A.; Frank, J. *Trends Biochem. Sci. (Pers. Ed.)* **1981**, *6*, 278.

(4) Anal. Calcd. for  $C_9H_8N_2O_2 \cdot 0.2H_2O$  ( $I_{ox}$ ): C, 60.13%; H, 4.71%; N, 15.57%. Found: C, 60.38%; H, 4.46%; N, 15.23%. Mass spectrum (EI mode),  $m/z$  ( $P^+$ ) 176.

(5) Alcock, N. W.; Benton, O. J.; Moore, P. *Trans. Faraday Soc.* **1970**, *66*, 2210.

is deemed thermodynamically unfeasible,<sup>11</sup> however. Regarding the slow enolization of  $\text{IH}_T$  to  $\text{IH}_{2T}$ , Ogata<sup>12</sup> and co-workers have observed rapid equilibrium addition of a sulfur nucleophile to a fused benzoquinone followed by slow base-catalyzed enolization to the substituted hydroquinone in aqueous media.

**Acknowledgment.** This research was supported by a Faculty Grant-in-Aid from Arizona State University, a Cottrell Research Grant from Research Corporation, the donors of the Petroleum Research Fund, administered by the American Chemical Society, and by an award from the National Cancer Institute, DHHS (PHS 1 R01 CA 36876-01).

(11) Eberson, L. *Acta Chem. Scand., Ser. B* 1984, B38, 439.

(12) Ogata, Y.; Sawaki, Y.; Isono, M. *Tetrahedron* 1970, 26, 1970.

## 6-Hydroxyanthranilic Acid: A New Shikimate Pathway Product Found in the Biosynthesis of Sarubicin A

Larry R. Hillis and Steven J. Gould\*<sup>1</sup>

Department of Chemistry, Oregon State University  
Corvallis, Oregon 97331

Received March 22, 1985

Sarubicin A, a quinoid antibiotic isolated from various strains of *Streptomyces*,<sup>2-4</sup> has been characterized as **1** on the basis of physical data.<sup>4,5</sup> Confirmation was provided by a recent total synthesis.<sup>6</sup> The  $^1\text{H}$  NMR spectrum and the nonaromatic portion of the  $^{13}\text{C}$  NMR spectrum of **1** have been assigned.<sup>7</sup> We now report that the quinone portion of **1** is biosynthesized from 6-hydroxyanthranilic acid, derived by an apparently new variation of the shikimate pathway.

Previous work at The Upjohn Co. had demonstrated that glucose **2** is the direct precursor to the tetrahydropyran portion of sarubicin A and had indicated a possible shikimate origin for the quinone ring.<sup>8</sup> Building on this foundation, we carried out a fermentation of *Streptomyces helicus* (UC-5837) in the presence of  $^{18}\text{O}_2$ . A 100-mL seed broth<sup>9</sup> in a 500-mL flask was inoculated with spores of *S. helicus* and incubated at 32 °C for 24 h in a rotary shaker (225 rpm). A 10-mL portion was then added to each of two production broths<sup>10</sup> (250 mL in 1-L Erlenmeyer flasks). These were connected in series via two sterile filters to a closed system containing a burette refillable with  $^{18}\text{O}_2$  (50%, obtained from Cambridge Isotopes, Inc.), a small air pump, and a  $\text{CO}_2$  trap (aqueous KOH). Air was circulated at 2 L/min while the fermentation flasks were shaken as described above. After 72 h the fermentation was stopped; the combined broths were adjusted to pH 3 (1 N HCl), filtered, saturated with  $(\text{NH}_4)_2\text{SO}_4$  (260 g), and extracted with three 500-mL portions of EtOAc. The extracts were dried ( $\text{Na}_2\text{SO}_4$ ), filtered, concentrated, and chromatographed on silica gel. Elution with 10% MeOH/ $\text{CHCl}_3$  gave 15.8 mg of pure **1a**.

(1) Career Development Awardee of the National Cancer Institute (CA00880), 1979-1984.

(2) Tresselt, D.; Reinhart, G.; Ihn, W.; Eckhardt, K.; Bradler, G. *Z. Chem.* 1980, 20, 147.

(3) Reinhardt, G.; Bradler, G.; Eckardt, K.; Tresselt, D.; Ihn, W. *J. Antibiot.* 1980, 33, 787-790.

(4) Slechta, L.; Chidester, C.; Rensser, F. *J. Antibiot.* 1980, 33, 919-923.

(5) The absolute stereochemistry was determined by chiroptical analysis: Eckardt, K.; Tresselt, D.; Ihn, W.; Kajtar, M.; Angyan, J.; Radics, L.; Hollos, M. *J. Antibiot.* 1983, 36, 976-979.

(6) Takeuchi, Y.; Sudani, M.; Yoshii, E. *J. Org. Chem.* 1983, 48, 4152-4154.

(7) Tresselt, D.; Eckardt, K.; Ihn, W.; Radics, L.; Reinhardt, G. *Tetrahedron* 1981, 37, 1901-1965.

(8) Slechta, L., private communication.

(9) The medium for the seed culture consisted of Pharmamedia, 25.0 g, glucose, 25.0 g, and tap water to 1.0 L. The pH was adjusted to 7.2 with 1 N NaOH. Slechta, L., private communication.

(10) The medium for the production culture consisted of glucose, 5.0 g,  $(\text{NH}_4)_2\text{SO}_4$ , 1.0 g,  $\text{CaCO}_3$ , 5.0 g, trace salts, 1.0 mL, and water to 1.0 L. The trace salts stock was made up of  $\text{MgSO}_4 \cdot 7\text{H}_2\text{O}$ , 200 g,  $\text{MnSO}_4 \cdot \text{H}_2\text{O}$ , 5.0 g,  $\text{ZnSO}_4 \cdot \text{H}_2\text{O}$ , 10.0 g,  $\text{FeSO}_4 \cdot 7\text{H}_2\text{O}$ , 6.0 g,  $\text{CoCl}_2 \cdot 6\text{H}_2\text{O}$ , 2.0 g, and deionized water to 1 L. Slechta, L., private communication.

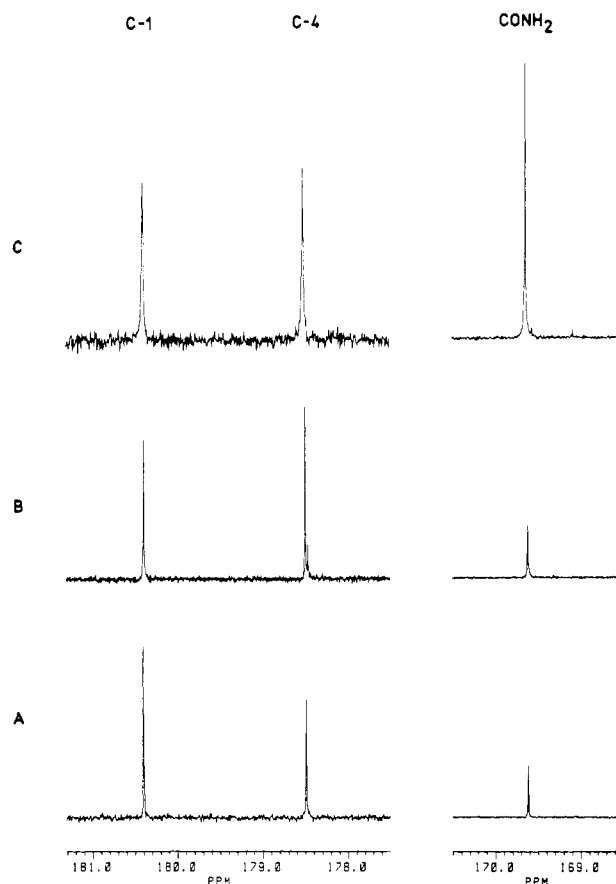


**Figure 1.** Waltz decoupled  $^{13}\text{C}$  NMR spectra, 100.6 MHz, of sarubicin A taken on a Bruker AM 400 spectrometer. (A) Natural abundance **1** (SW = 22 727 Hz, SI = TD = 64 K, AQ = 1.44 s, NS = 24 000, PW = 36°). (B)  $^{18}\text{O}$ -labeled **1a** (SW = 25 000 Hz, SI = TD = 128 K, AQ = 2.62 s, NS = 25 927, PW = 36°). (C)  $^{13}\text{C}$ -labeled **1b** (NS = 28 000, other parameters same as for (A)). The amplitude for the 177.5-181.4 ppm region is 5 times that of the 168.5-170.5 ppm region in all three spectra.

Examination of the EI mass spectrum of **1a** indicated that one  $^{18}\text{O}$  label had been incorporated, and fragments<sup>7</sup> at  $m/z$  252, 235, and 207 led us to believe that the label was in one of the quinone carbonyls. In order to identify the precise location of the label, we intended to use the expected isotope shift of the  $^{13}\text{C}$  NMR resonance.<sup>11</sup> However, it was first necessary to overcome the problem of carbonyl resonances 7-15 Hz wide that were encountered repeatedly with various samples of **1**. Fortunately, when a warm, dilute aqueous solution of **1** was filtered through a small portion of Chelex, interfering paramagnetic ions were apparently removed. After lyophilization, the 100-MHz  $^{13}\text{C}$  NMR spectrum of a portion of the sample in  $\text{Me}_2\text{SO}-d_6$  gave excellent narrow lines (Figure 1A). This was repeated for **1a** and the 178.50 ppm resonance was found to be accompanied by a smaller peak 0.03 ppm (3.45 Hz) upfield (Figure 1B).

To assign the  $^{13}\text{C}$  NMR resonances of the quinone ring, a second portion of the deionized natural abundance sample was exchanged 3 times with ethanol- $d_1$ , dried thoroughly, and combined with an unexchanged, deionized sample in  $\text{Me}_2\text{SO}-d_6$ . From the deuterium-induced isotope shifts of the  $^{13}\text{C}$  NMR resonances<sup>12</sup> thus obtained, the resonances at 180.0 and 178.5 ppm could be unequivocally assigned to C-1 and C-4, respectively. The C-4 resonance showed five additional lines (upfield shifts of 0.01, 0.03,

(11) Risley, J. M.; Van Etten, R. L. *J. Am. Chem. Soc.* 1979, 101, 252. Vederas, J. C. *Ibid.* 1980, 102, 374. Vederas, J. C. *J. Chem. Soc., Chem. Commun.* 1980, 183.

(12) Pfeiffer, P. E.; Valentine, K. M.; Parrish, F. W. *J. Am. Chem. Soc.* 1979, 101, 1265. Newmark, R. A.; Hill, J. R. *Org. Magn. Reson.* 1980, 13, 40. Christofides, J. C.; Davies, D. B. *J. Chem. Soc., Chem. Commun.* 1983, 324. Reuben, J. *J. Am. Chem. Soc.* 1983, 105, 3711.